Engineering and Technology Journal
Journal homepage: https://etj.uotechnology.edu.iq

The Structural and Optical Investigation of Grown GaN Film on Porous Silicon Substrate Prepared by PLD

Haneen D. Jabbar[a], Makram A. Fakhri[a*], Mohammed J. AbdulRazzaq[a], Subash C. B. Gopinath[b,c,d]

[a] Laser and Optoelectronics Engineering Dept., University of Technology-Iraq, Alsina'a street, 10066 Baghdad, Iraq.
[b] Institute of Nano Electronic Engineering, University Malaysia Perlis, 01000 Kangar, Perlis, Malaysia.
[c] Faculty of Chemical Engineering Technology, Universiti Malaysia Perlis, 02600 Arau, Perlis, Malaysia.
[d] Centre of Excellence for Nanobiotechnology and Nanomedicine (CoExNano), Faculty of Applied Sciences, AIMST University, Semeling, 08100 Kedah, Malaysia.
*Corresponding author Email: makram.a.fakhri@uotechnology.edu.iq

HIGHLIGHTS

- Grown GAN thin film had a hexagonal crystalline structure and high-intensity peak at the (002) plane.
- The absorption spectrum of grown GaN film showed a high absorbance at a UV spectrum of 302.88, 435.26 nm.
- Three methods relations were used to estimate the optical energy gap of prepared P-Si substrate and grown GaN film.
- The optical energy gap of the P-Si substrate was 2.1 eV, while the grown GaN thin film had a multi-optical energy gap of 3.3 and 1.6 eV.

ARTICLE INFO

Handling editor: Evan T. Salim

Keywords:
GaN;P-Si; Etching; Pulsed Laser deposition Optical Properties.

ABSTRACT

The optical properties of a grown gallium nitride (GaN) thin film on a porous silicon (P-Si) substrate was investigated. A Photo-electrochemical etching method was used to synthesize the Psi substrate, and a physical deposition method (pulsed laser deposition) of 1064 nm Q-switch Nd: YAG laser with a vacuum of 10^{-2} mbar was used to grow a thin layer of GaN on a prepared P-Si substrate. X-Ray diffraction displayed that GaN film has a high crystalline nature at the (002) plane. The photoluminescence of GaN film exhibited ultraviolet PL with a peak wavelength of 374 nm corresponding to GaN material and red PL with a peak wavelength of 730 nm corresponding to Psi substrate. The absorption coefficient of the P-Si substrate and grown GaN thin film was obtained from the absorption calculation of UV-Vis diffused spectroscopy at ambient temperature in the 230–1100 nm wavelength range. Extinction coefficients, optical energy gap, and refractive index of both the P-Si substrate and the grown GaN thin film have been determined, respectively. The direct optical energy gaps of both the P-Si substrate and grown GaN have also been determined using three methods: Plank's relation with photoluminescence (PL) spectroscopy, Tauc'relation, and Kubulka-Munk argument with Uv-Vis diffused spectroscopy. It was observed that the optical energy gap of the P-Si substrate was 2.1 eV, while the grown GaN thin film had a multi-optical energy gap of 3.3 eV and 1.6 eV. A good agreement has been obtained between these mentioned methods.

1. Introduction

Nowadays, Gallium Nitride (GaN) is one of the III-V nitride semiconductor materials with a hexagonal wurtzite structure that has unique optical properties with a wide tunable direct band-gap of 3.4 eV [1-3]. This makes it possible to make optoelectronic devices that work with UV and visible light, like LEDs, LDs, photodiodes, and UV detectors [4-6]. Furthermore, GaN has high-rise electron mobility, chemical stability, and great luminescence efficiency [7]. Moreover, GaN has thermal conductivity and high breakdown strength [8, 9]. All these advantages lead to fabricating of optoelectronic devices based on GaN with high frequency/temperature and low intrinsic noise/dark current/sensitivity to ionizing radiation to play an important role in industrial, military, and space applications [10-12].

The techniques used for GaN film preparation and the chosen parameters significantly impact the optical properties and electrical characteristics of GaN film [13, 14]. Therefore, in recent years, multiple procedures, including molecular beam epitaxy, metalorganic chemical vapour deposition, and pulse laser deposition (PLD), have been employed to produce better-quality thin-film GaN [15,16]. Moreover, each technique has advantages for growing GaN thin films at high vacuum levels, a

http://doi.org/10.30684/etj.2022.135733.1281
Received 05 September 2022; Accepted 22 October 2022; Available online 12 November 2022
2412-0758/University of Technology-Iraq, Baghdad, Iraq
This is an open access article under the CC BY 4.0 license http://creativecommons.org/licenses/by/4.0

faster growth rate, and low substrate temperature [17]. Thin films made by PLD often don't come apart because the substrate and GaN layer has strong crystalline lattice matches and the conditions for growth are right [18].

Using porous silicon (P-Si) substrate instead of silicon (Si) has been intensely studied by researchers since it was reported for visible photoluminescence (PL) by Canham in 1990. According to Canham, P-Si has many uses in producing optoelectronic devices such as photodiodes, LEDs, and sensors [19]. Because of its excellent thermal and mechanical properties, low cost, basic absorption edge transitioning into the short wavelength, and large surface area, P-Si is used in these optoelectronic devices [20].

In this work, the PLD method was utilized to grow GaN film on a Psi substrate because of its simplicity, versatility, and rapid film production with a strong forward-directed plume of material that can be deposited with low pollution and specific stoichiometry. An Nd: YAG laser, a solid-state laser with a wavelength of 1064 nm, was used to grow GaN on a Psi using laser energy of 1000 mJ and a vacuum pressure of 10^{-2} Torr. Three methods were based on measuring the optical energy gap of both prepared Psi and grown GaN films. This study examined the structural, spectroscopic, and optical properties of a thin film of grown GaN.

2. Materials

The materials and instuments used to prepare Psi substrate and GaN thin film were listed in Table 1.

Table 1: Materials and instuments used to prepare Psi substrate and GaN thin film

Materials and Instuments	Origion
GaN powder	Luoyang Advanced Material Company, 99.9% of high impurity, China
Silicon wafer	University Wafer, Inc., n-type, 500µm thickness, 0.001-0.005 Ω/cm electrical resistivity, and (100) orientations), USA
Diode laser	Tongtool Company, infrared wavelength of 660 nm and 100 mW power, China
DC power supply	Jiuyuan, 0-30 V, China
Digital multimeter	Victor Company, VC97, China
Beam expander	Carman Haas Company, 10x magnification, China
Hydrofluoric acid	Thomas Baker Company, 48% concentration, Germany
Ethanol	Honeywell Company, 99.9% concentration, Germany
platinum rode	95% purity, Turkey
Teflon cell	made of Teflon material with an electrolyte volume of 18 ml and stainless steel contact in the cell
Nd: YAG laser	uangzhou Dany Optical Technology CO., Ltd, China
X-ray diffraction	XRD6000 Shimadzu Company, Japan
Ultra Violet- Visible diffuse reflectance spectrometer	Avantes DH-S-BAL-24048 UV-Vis, wavelength range from 230 – 1100 nm, Netherlands,

3. Experimental Work

3.1 Preparing Porous Silicon Substrate

A top-down approach of the photo-electrochemical etching method assisted by a diode laser was used to fabricate a porous silicon (P-Si) substrate at room temperature. Silicon was cut into small pieces of (1x1) cm^2 and cleaned by an ultrasonic device for 10 minutes with absolute ethanol to remove impurities, then for 12 minutes with distilled water, and lastly by blowing with dry air. Next, the silicon wafer was dipped in the synthesized etching electrolyte solutions, which contained 1:2 ratios of concentrated hydrofluoric acid (48%) and ethanol (99.9%) for 10 minutes with a 10 mA/cm^2 current density. A Teflon cell was used with the platinum electrode as a cathode and a silicon wafer as an anode, as shown in Figure 1.

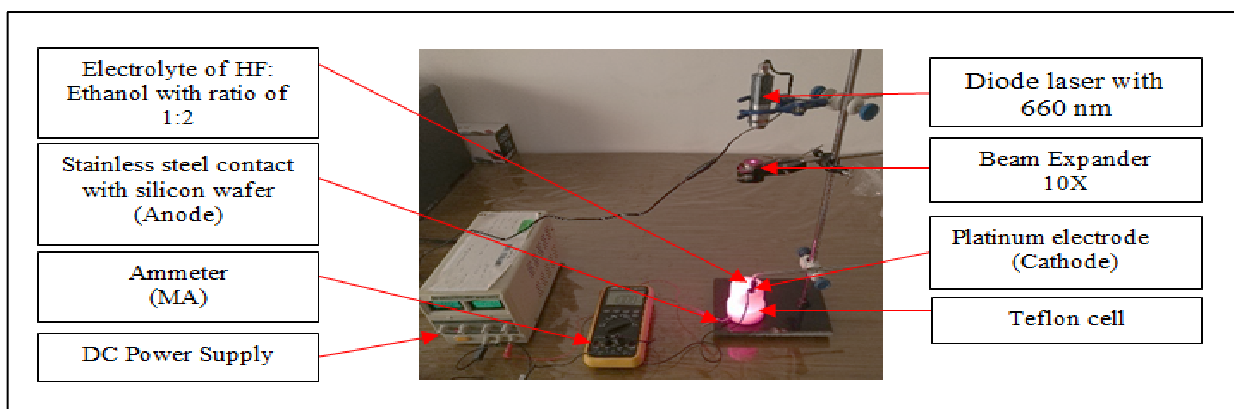

Figure 1: The process of photo-electrochemical etching with laser assistance to prepare the P-Si substrate

3.2 Preparing GaN Target

A pellet of gallium nitride (GaN) was prepared by pressing GaN powder with a hydraulic press of 15 kg cm^2. The obtained GaN sample of 5 gm in weight, 2 cm in diameter, and 0.5 cm in thickness are shown in Figure 2.

Figure 2: The GaN pellet

3.3 Grown GaN Thin Film on P-Si Substrate by PLD

Using the pulse laser deposition technique (PLD), a Q-switching Nd: YAG laser with a vacuum pressure of 10^{-2} mbar (Guangzhou Dany Optical Technology CO., Ltd, China) was used to grow a thin layer of GaN onto a Psi substrate as indicated in Table 2.

Table 2: The practical parameters of the PLD method

Laser Parameters	The Values
Laser wavelengths	1064 nm
Pulse energy	1000 mj
Pulse duration	7 ns
Frequency	3 Hz
Repetition rate	300 Hz
Power supply	220 V
substrate	porous silicon
substrate temperature	300℃

The GaN target and Psi substrate were placed well within the PLD system's vacuum chamber. Also, the GaN target was placed on a rotating base at an angle of 45°. The P-Si substrate is fixed horizontally at 5 cm just above the pressed GaN target. The Q-switch Nd: YAG laser was subjected to the GaN target by a focused lens of 12 cm focal length to perform a strong forward-directed plume of GAN material that can be deposited on a Psi substrate with low pollution and specific stoichiometry, as shown in Figure 3.

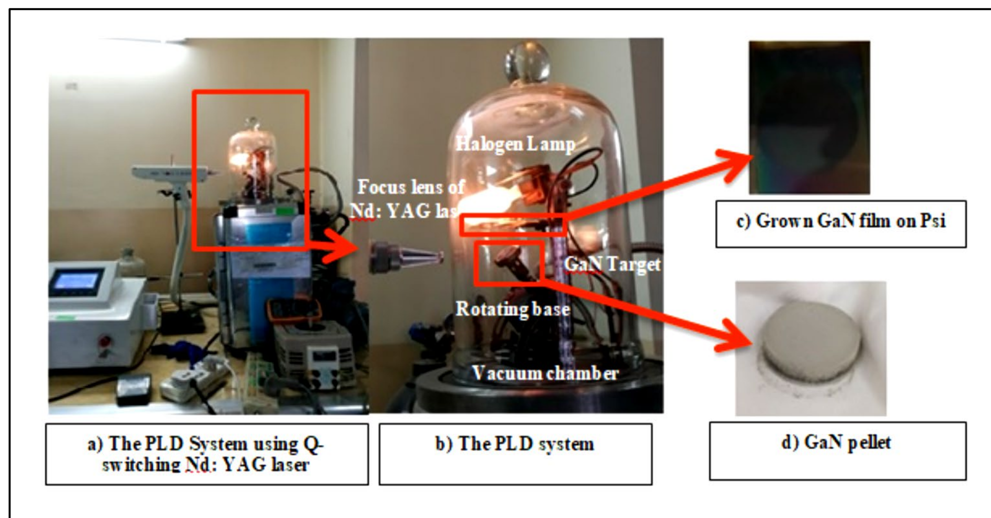

Figure 3: Grown GaN film on Psi substrate using only 1000 mj laser energy (a to d)

The structural characteristics of the Psi substrate and grown GaN film were investigated using X-ray diffraction (XRD) from Japan (XRD6000 Shimadzu Company) with copper radiation of 1.54060 Å. In addition, the spectroscopic properties were investigated using a spectroscopic system from the United States of America (Perkin Elmer Company) with a wavelength range of 200–800 nm to measure the photoluminescence (PL) at room temperature. Moreover, a UV-Vis diffuse reflectance UV-VIS spectrometer (Avantes DH-S-BAL-24048 UV-Vis, Netherlands) with a wavelength range from 230–1100 nm was employed to measure the optical properties of the reflectance.

4. Results and Discussion

4.1 Structural Characteristic Analysis

X-ray diffraction (XRD) study was carried out for the prepared P-Si substrate and grown GaN film to find the structural properties, as shown in Figure 4 a and b. As shown in Figure 4 a, two prominent XRD peaks were observed at 2theta = 33 and 69.23 degrees, corresponding to the (200) and (400) planes that related to the P-Si substrate. These peaks were indexed and consistent with the silicon standard's diffraction data (JCPDS card 27-1402), according to Kang [21].

Three XRD peaks were observed at 2theta equal to 33.16, 59.12, and 61.84 degrees, corresponding to (002), (110), and (103) planes that related to GaN material, as shown in Figure 4 b. These peaks were in conformity and accordance with the GaN standard's diffraction data (JCPDS card 01-074-0243) of a hexagonal crystalline structure. It's worth noting that the GaN peak at (002) shows a high sharp peak due to the smaller crystal size [22].

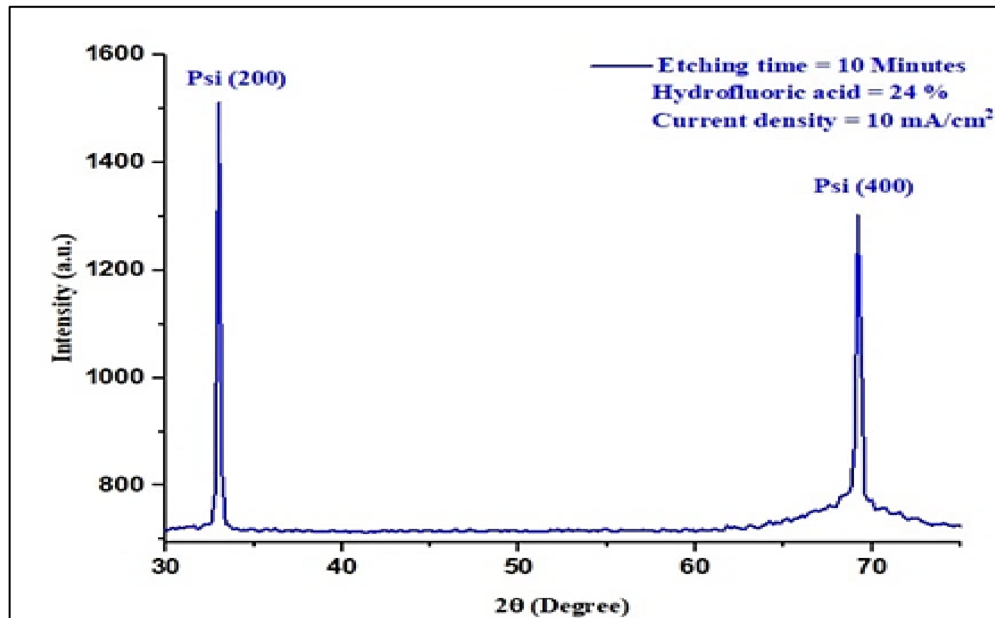

(a)

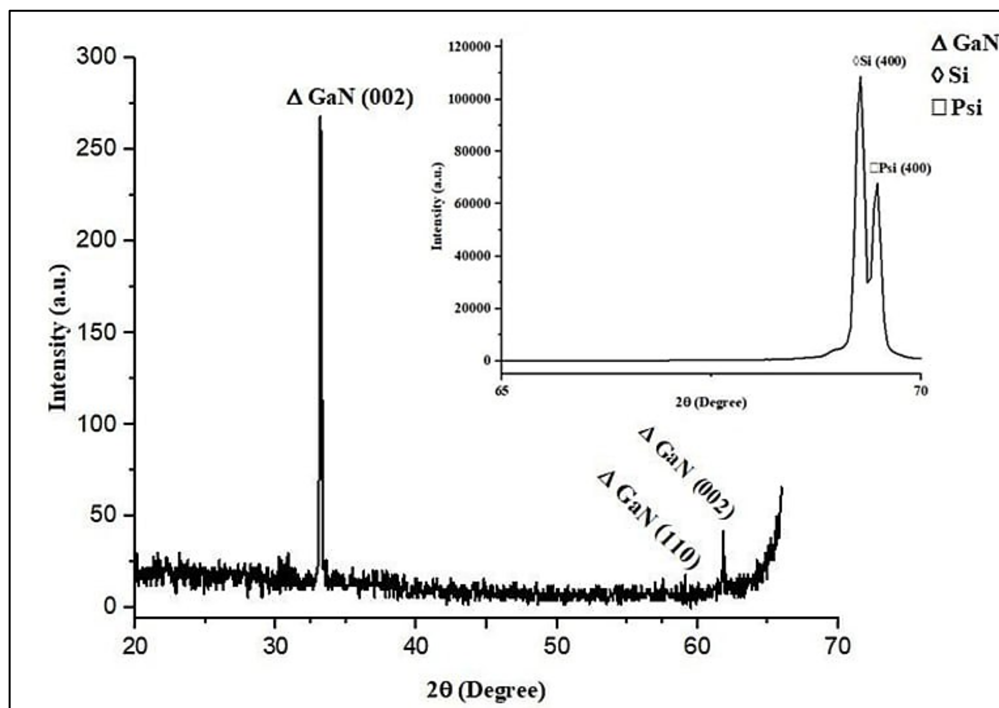

(b)

Figure 4: XRD pattern of a) Psi substrate, b) Grown GaN film on Psi substrate

The crystal size was calculated for the Psi substrate and grown GaN thin film from the XRD pattern as shown in Table 3 based on the Scherrer Equation [23]:

$$D = 0.94\lambda/\beta \cos\theta \quad (1)$$

Where λ is the incident X-ray wavelength (λ = 1.5406 Å), β is the full width at half maximum, and θ is the diffraction angle.

Also, the interplanar distance d was computed as shown in Table 3 by using the following formula [24]:

$$d = n\lambda/2\sin\theta \quad (2)$$

Where d is the Interplanar spacing in A°, K is a constant taken to be 0.9, λ is the x-ray wavelength (Wavelength of CuK_{α} = 1.54060 A°), β is the full-width half maximum of the XRD pattern, θ is Bragg's angle in degree, and n is diffraction order.

Table 3: XRD for the Psi substrate and grown GaN thin film

Structure	hkl	2θ (Deg.)	d(nm)	FWHM (Deg.)	D(nm)
Psi substrate	(200)	33	0.27	0.28	29.10
	(400)	69.23	0.13	0.31	30.88
GaN thin film	(002)	33.16	0.27	0.18	46.10
	(110)	59.12	0.15	0.06	152.41
	(103)	61.84	0.15	0.04	231.80

4.2 Spectroscopic Properties Analysis

The photoluminescence (PL) spectra of the prepared n-type P-Si using 10 minutes of etching time and 10 mA/cm^2 current density were obtained, as shown in Figure 5 a. It can be observed that the synthesized Psi substrate exhibited yellow visible PL with a peak wavelength of 590 nm, according to Wang [25]. This emission was caused by the surface states and quantum confinement that developed on the P-Si following the photo-electrochemical etching process, as determined by [26].

Also, the photoluminescence (PL) spectra of grown GaN film on a P-Si substrate were performed, as shown in Figure 5 b. It can be noticed that the grown GaN film exhibited ultraviolet PL with a peak wavelength of 374 nm corresponding to GaN material and red PL with a peak wavelength of 730 nm corresponding to Psi, according to Wang [25]. According to Li et al., the photoluminescence spectral and energy gap of the prepared porous silicon substrate have been shifted after the deposition of GaN material on it due to the changes in the surface chemistry achieved [27].

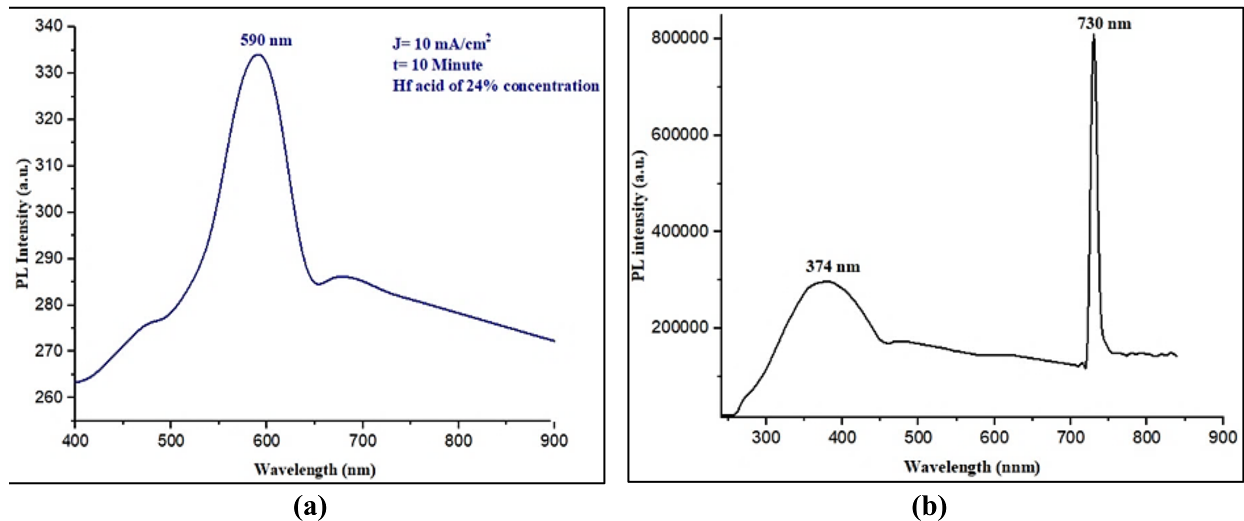

Figure 5: Photoluminescence of a) Psi substrate, b) Grown GaN film on Psi substrate

Figures 6 a and b show the energy gap (Eg) vs. wavelength for prepared Psi substrate and grown GaN film. It could be observed that the energy gap of P-Si was 2.1 eV before deposition, as shown in Figure 6 a. Two energy gaps appeared for grown GaN film: 3.3 eV, which corresponds to GaN material, and 1.6 eV, which corresponds to P-Si substrate after PLD as shown in Figure 6 b. It's observed that the P-Si substrate was reduced after the deposition of GaN material on it. The energy gap was then calculated using Eq. (3) [28].

$$E_g(eV) = h\upsilon/\lambda = 1.24/\lambda\,(nm) \quad (3)$$

Where, E_g is the energy gap, hυ is the photon energy, h is Planck's constant ($6.62*10^{-34}$ J. Sec), υ is the photon's frequency, λ is the photon's wavelength.

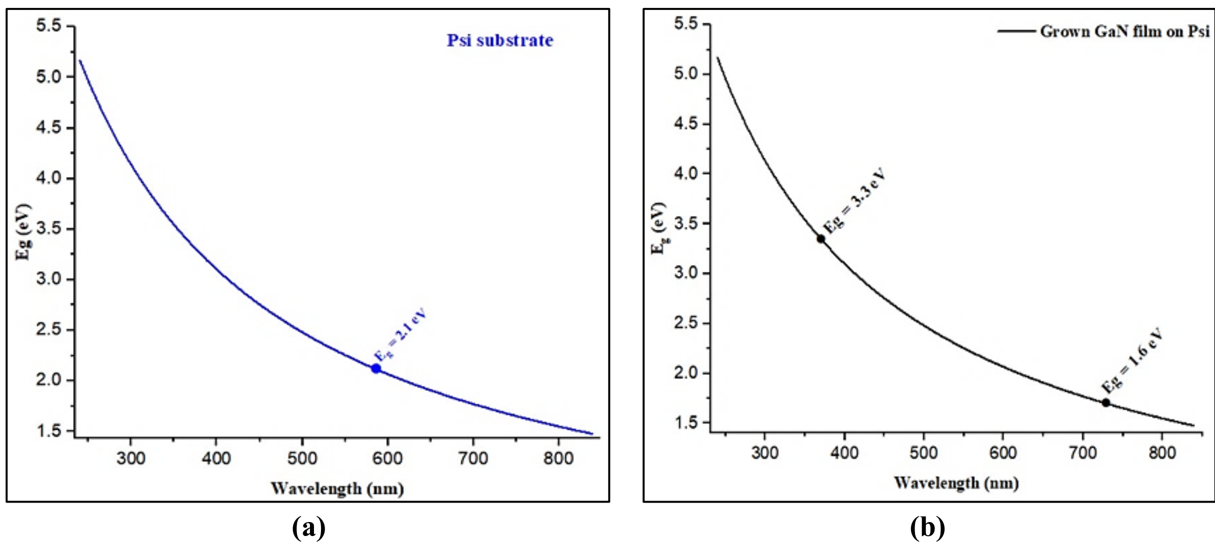

Figure 6: Energy gaps Vs. wavelength using plank equation for a) Psi substrate, b) Grown GaN film on Psi substrate

4.3 Optical Properties Analysis

The optical properties of any material rest on the preparation methods and conditions, morphological, structural surface, doping, and interaction with the neighboring environment. So, the spectral behavior of the absorption coefficient of any semiconducting material can be studied to learn more about the electronic states in the high-energy part of the optical absorption spectrum. The lower energy part of the spectrum is made up of atomic vibrations [29].

Several optoelectronic devices, including photodiodes, sensors, and LEDs, rest on the optical absorption of the material. Therefore, studying the optical absorption spectra and the optical absorption coefficient (α) is important. The optical properties such as reflectance R (λ) and absorbance A (λ) of both the Psi substrate and grown GaN thin film were performed using UV-Vis diffuse reflectance spectroscopy (Avantes DH-S-BAL-2048UV-Vis, Netherlands) in a wavelength range of 230–1100 nm as shown in Figures 7, and 8.

The absorption spectrum of the prepared Psi substrate showed many peaks at 309.42, 448.17, 513.08, and 543.34 nm, as shown in Figure 7 a. Whearas, Figure 7 b shows the absorption spectrum of grown GaN film, which shows many peaks at 302.88, 435.26 nm. So it's noticed that the grown GaN film is blue-shifted with high absorption in the UV range, which means the electrons will move from the valance band to the conduction band in this spectrum region.

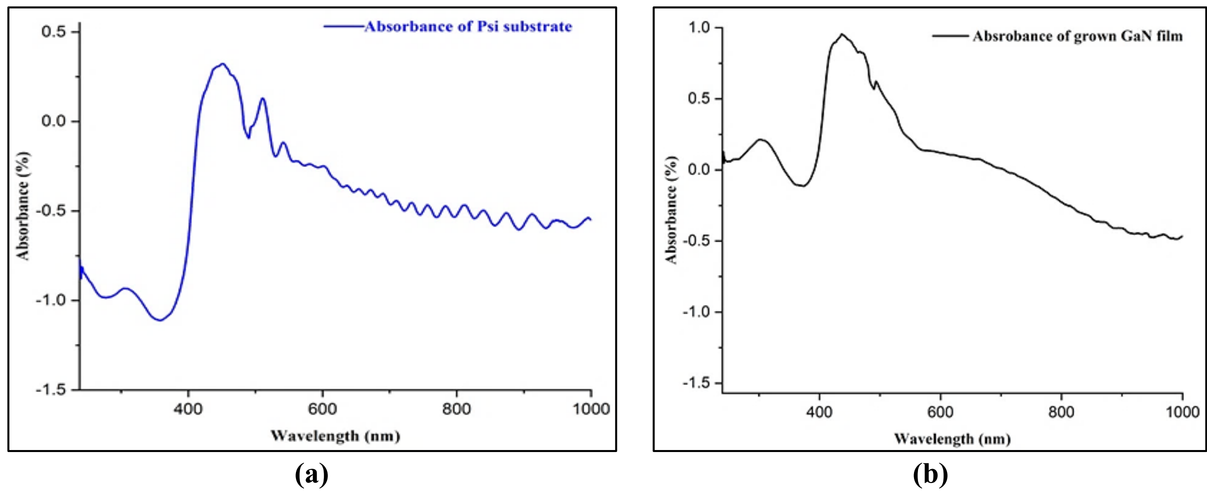

Figure 7: Absorption spectra of a) Psi substrate, b) Grown GaN film on Psi substrate

Figure 8 a shows low reflection peaks of P-Si were observed at 277.3 and 360.99 nm due to the high absorption peaks in the UV region spectrum. Furthermore, a high sharp reflection peak was observed at 1184.59 nm. Figure 8 b shows a high reflection peak of grown GaN film was observed at 118.59 nm due to the Psi substrate, and low reflection peaks were observed at 1158.68 and 373.99 nm due to the absorption effects of the GaN material in the UV region.

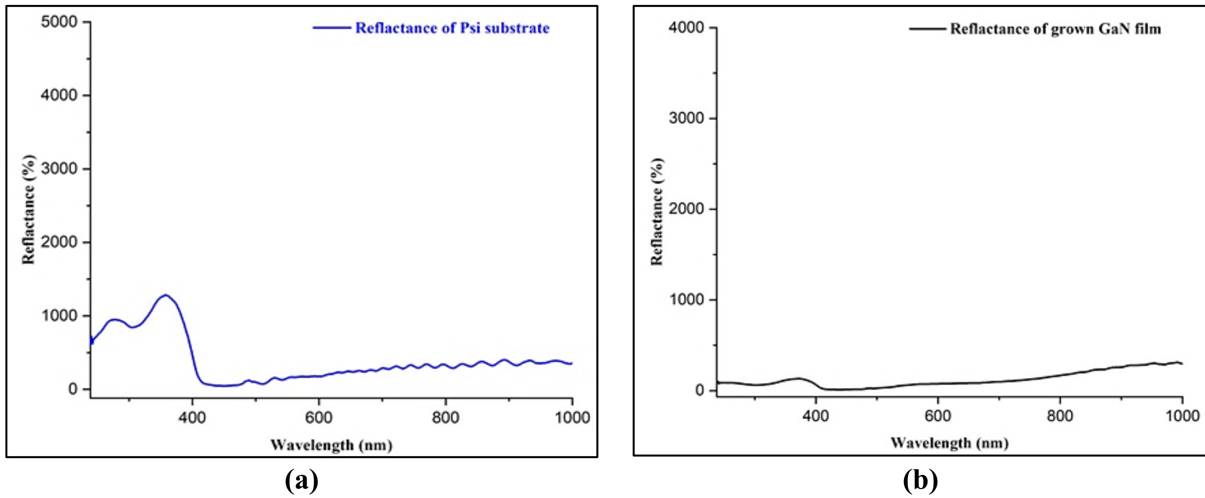

Figure 8: Reflection spectra of a) Psi substrate, b) Grown GaN film on Psi substrate

The absorption coefficient, extinction coefficient (K), and refractive index of both Psi substrate and grown GaN film (n_s and n_f), optical energy gap (E_g) respectively were calculated with the aid of the following Equations [30] :

$$\alpha = 2.303\ A/t \quad (4)$$

α is the absorption coefficient, A is the absorbance value at a particular wavelength range, and t is the thickness.

$$K = \alpha\, \lambda / 4\pi \quad (5)$$

α is the calculated absorption coefficient as mentioned in Eq. (4), λ is the wavelength of U-Vis spectroscopy ranging from 230 to 1100 nm.

$$n_s = \sqrt{\frac{4R}{(R-1)} - K^2} - \frac{(R+1)}{(R-1)} \quad (6)$$

n_s is the refractive index of the prepared Psi substrate, R is the reflectance of Psi substrate, and K is the calculated extinction coefficient, as mentioned in Eq. (6)

$$n_f = n_s \left(\frac{1+\sqrt{R}}{1-\sqrt{R}}\right)^{0.5} \quad (7)$$

n_f is the refractive index of grown GaN thin film, n_s is the refractive index of the prepared Psi substrate that is calculated as mentioned in Eq. (4), and R is the reflectance of the grown GaN thin film.

Figure 9 a, b show the refractive index vs. the wavelength for P-Si substrate and grown GaN film, respectively. Figure 9 a shows the refractive index of the P-Si substrate (n_s), which has a stable value of 0.999 in the UV region, starts to decrease clearly to 0.978 at 377 to 451 nm, then increases gradually to 0.991 at 490 nm, and decreases again to 0.986 at 512 nm. While Figure 9 b shows the refractive index of grown GaN film (n_f) that has a stable value of 0.991 in the UV region, then decreases slightly to 0.796 at 438 nm, then becomes a stable value of 0.999 as the wavelength increases.

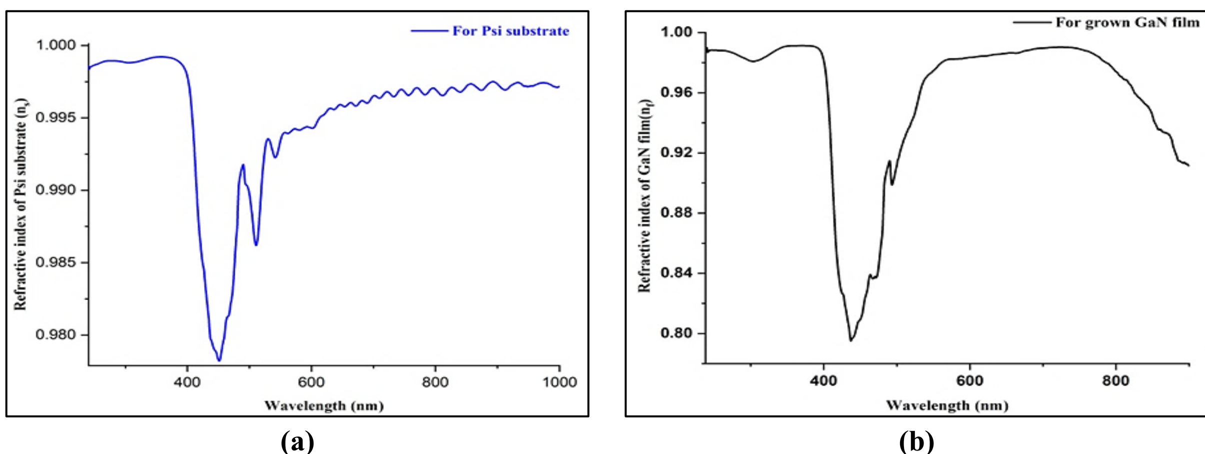

Figure 9: Refractive index of a) Psi substrate, b) Grown GaN film on Psi substrate

The energy gaps of the prepared Psi substrate and grown GaN film were calculated using three relations; Plank's relation, Tauc's relation, and the Kubelka-Munk argument that describe the behavior of light traveling inside a light-scattering Psi and grown GaN film. Furthermore, the first relation used to estimate the energy band gaps was Plank's relation, as mentioned in Figure 6a, b. The second relation that depended on estimating the band gaps was Tauc's relation, as shown in Figure 10a, b by plotting the graph of the square product of the absorption coefficient and photon energy $(\alpha h\upsilon)^2$ versus photon energy (E_g) [31].

$$(\alpha h\upsilon)^2 = A(h\upsilon\text{-}E_g) \tag{8}$$

hυ is the optical photon energy where h is plank's constant ($6.62*10^{-34}$ Joule. Sec), υ is the photon frequency, and A is constant and also named the band tailing parameter. B is the energy gap based on the density of states concept put out by Mott and Davis that is placed between localized states close to the mobility boundaries [32]. The relationship between $(\alpha h\upsilon)^2$ and incident photon energy for P-Si substrate and grown GaN film is shown in Figure 10 a, b. Figure 10 a shows the energy band gaps of the P-Si substrate to be 2.3, 3, and 3.2 eV. Figure 10 b shows the energy band gaps of grown GaN film to be 2.25, 3, and 3.5 eV.

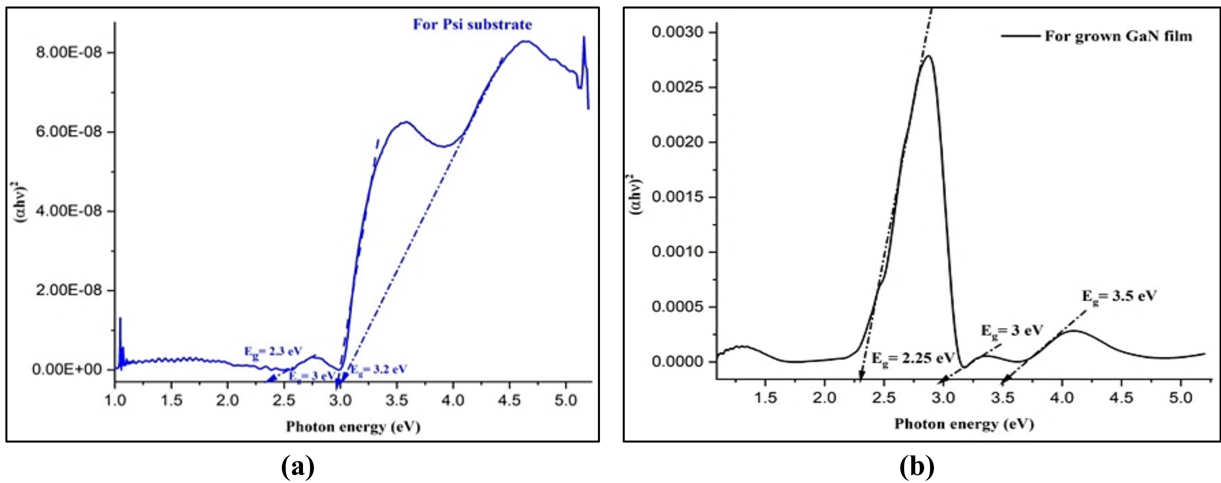

(a) **(b)**

Figure 10: Dependence of (αhυ) 2 upon incident photon energy for a) Psi substrate, b) Grown GaN film on Psi substrate byusing Tauc's relation

The Third relation that depended on estimating the energy band gaps were Kubelka-Munk (K-M) argument, as shown in the following equation [33]:

$$F_{KM} = \frac{(1-R^2)}{2R} \tag{9}$$

F_{KM} is Kubelka-Munk function, and R is the reflectance obtained from UV-Vis diffused spectroscopy. Furthermore, Figure 11a, b show the relation between the Kubelka-Munk function and incident photon energy for the P-Si substrate and grown GaN film. Figure 11 a shows the energy band gaps of the P-Si substrate obtained from the graph to be 2.9 and 3 eV. Whereas Figure 11 b shows the energy band gaps of grown GaN film obtained from the graph to be 2.1 and 3 eV.

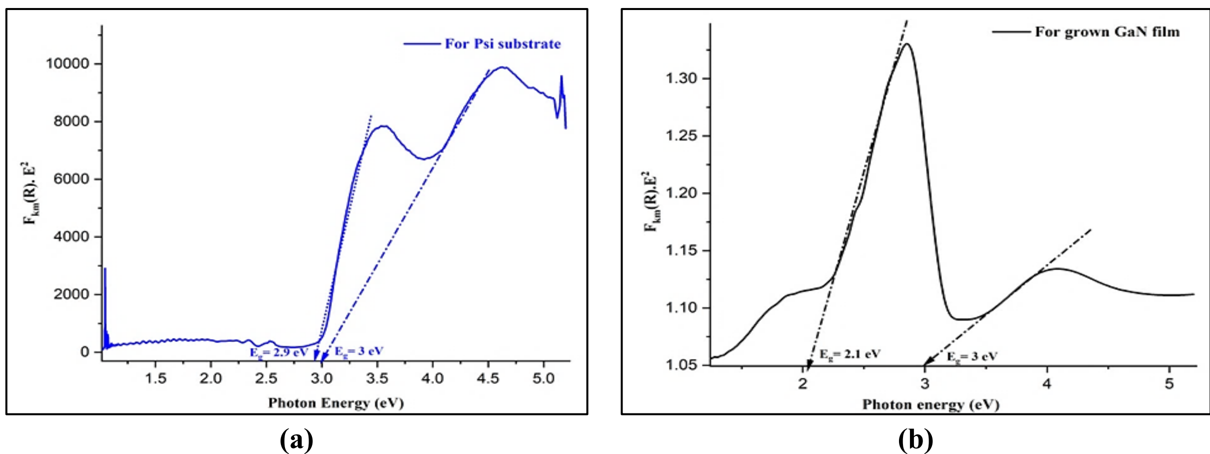

(a) **(b)**

Figure 11: Optical energy band gaps Vs. the photon energy of a) Psi substrate, b) Grown GaN film on Psi substrate by using Kubelka-Munk (K-M) argument

5. Conclusion

The GaN nanostructure thin film was grown physically using the pulsed laser deposition method at 1000 mJ laser energy and 1064 nm laser wavelength. The results show that the XRD of grown GaN film shows a high-intensity peak at the (002) plane that relates to the hexagonal wurtzite structure. The absorbance of the prepared thin film was increased by 64% and blue-shifted after the deposition of GaN material. Furthermore, the refractive index of the prepared thin film decreased from 0.97 to 0.79 in the UV region. Still, in the other spectrum region, it decreased from 0.998 to 0.987 after the deposition of GaN material. Furthermore, all-optical parameters of prepared P-Si and grown GaN films were calculated as reflectance, absorbance, absorption coefficient, extinction coefficient, refractive index, and energy band gaps using a computer program based on solving Murmann's exact equation. Based on the three relations of Plank, Tauc, and Kubalka-Munk, the difference between the estimated energy band gaps for a P-Si substrate and a grown GaN film was approximate. In photodetection applications of UV radiation, such as enhanced communication, ozone sensing, and air purification, the grown GaN/Psi nanostructure has been a potential possibility. It is also used in civilian and military applications, like warning missiles, detecting chemical and biological substances, and finding flames.

Author contribution

All authors contributed equally to this work.

Funding

This research received no specific grant from any funding agency in the public, commercial, or not-for-profit sectors.

Data availability statement

The data that support the findings of this study are available on request from the corresponding author.

Conflicts of interest

The authors declare that there is no conflict of interest.

Reference

[1] F. Lu, H. Wang, M. Zeng, L. Fu, Infinite possibilities of ultrathin III-V semiconductors: Starting from synthesis. Iscience, 25 (2022) 103835. https://doi.org/10.1016/j.isci.2022.103835

[2] Y.Wu, X. Liu, A.Pandey, P. Zhou, W.J Dong, et.al. III-Nitride Nanostructures:Emerging Applications for Micro-LEDs, Ultraviolet Photonics, Quantum Optoelectronics, and Artificial Photosynthesis, Prog.Quantum Electron., 85 (2022)100401. https://doi.org/10.1016/j.pquantelec.2022.100401

[3] H.D. Jabbar, M.A. Fakhri, M.J. AbdulRazzaq, Gallium Nitride–Based Photodiode: A review. Mater. Today: Proc., 42 (2021) 2829-2834. https://doi.org/10.1016/j.matpr.2020.12.729

[4] Z.T. Li, H.W. Zhang, J.S Li., , K. Cao, Z. Chen, et.al . Perovskite-Gallium Nitride Tandem Light-Emitting Diodes with Improved Luminance and Color Tunability, Adv. Sci., 9 (2022) 2201844. https://doi.org/10.1002/advs.202201844

[5] H.A.A.A. Amir, M.A. Fakhri, A.A. Alwahib, E.T. Salim, F.H. Alsultany, et.al. Synthesis of gallium nitride nanostructure using pulsed laser ablation in liquid for photoelectric detector. Mater. Sci. Semicond. Process., 150 (2022)106911. https://doi.org/10.1016/j.mssp.2022.106911

[6] B. Wang, S. Liang, J. Yu, F. Xu, D. Zhang, et.al. Cascade GaN-based micro-photodiodes for photonic integration. J. Phys. D: Appl. Phys., 55 (2022) 404004. https://doi.org/10.1088/1361-6463/ac818a

[7] F. Wang, L. Li, H. Tang, Y. Hu, Effects of thickness and orientation on electromechanical properties of gallium nitride nanofilm: A multiscale insight. Comput. Mater. Sci., 203 (2022) 111122. https://doi.org/10.1016/j.commatsci.2021.111122

[8] D. Zhang, L. Gao, Y. Tian, S. Zhang, Y. Du, et.al. Structural Design and Physical Properties of Gallium Nitrides under High Pressures. J. Phys. Chem. C.,126 (2022) 7773-7777. https://doi.org/10.1021/acs.jpcc.2c01801

[9] B. Ul Haq, S. AlFaify, R. Ahmed, , F.K. Butt, K. Alam, et.al. Structural, electronic, and optical properties of the pressure-driven novel polymorphs of gallium nitride: first-principles investigations. Int. J. Energy Res., 46 (2022) 2361-2372. https://doi.org/10.1002/er.7313

[10] B.J. Galapon, A.J. Hanson, D.J. Perreault, Measuring dynamic on resistance in GaN transistors at MHz frequencies. In 2018 IEEE 19th Workshop on Control and Modeling for Power Electronics (COMPEL) IEEE., 2018,1-8 . https://doi.org/10.1109/COMPEL.2018.8460051

[11] J. Gallagher, O. Aziz, M.High Frequency Inductors for GaN Applications: Construction Analysis and Efficiency Comparison. In PCIM Europe 2019; International Exhibition and Conference for Power Electronics, Intelligent Motion, Renewable Energy and Energy Management , VDE.2019, 1-7.

[12] F. Bartoli, T. Aubert, M. Moutaouekkil, J. Streque, P. Pigeat, et.al. AlN/GaN/Sapphire heterostructure for high-temperature packageless acoustic wave devices. Sens. Actuator A Phys. 283 (2018) 9-16. https://doi.org/10.1016/j.sna.2018.08.011

[13] K. Du, Z. Xiong, L. Ao, L. Chen, Tuning the electronic and optical properties of two-dimensional gallium nitride by chemical functionalization. Vacuum., 185 (2021)110008. https://doi.org/10.1016/j.vacuum.2020.110008

[14] A.K. Viswanath, Optical Properties of Gallium Nitride Nanostructures, In Encyclopedia of Nanoscience and Nanotechnology, 8 (2004) 179-217.

[15] X. Wang, A. Yoshikawa, Molecular beam epitaxy growth of GaN, AlN and InN, Prog. Cryst. Growth Charact. Mater., 48 -49 (2004) 42-103. https://doi.org/10.1016/j.pcrysgrow.2005.03.002

[16] Y. Zhang, Z. Chen, W. Li, A.R. Arehart, S.A. Ringel, Metalorganic Chemical Vapor Deposition Gallium Nitride with Fast Growth Rate for Vertical Power Device Applications, Phys. Status Solidi A, 218 (2021) 2000469. https://doi.org/10.1002/pssa.202000469

[17] K-C. Shen, M.C. Jiang, H.R. Liu, H.H. Hsueh, Y.C. Kao, Pulsed laser deposition of hexagonal GaN-on-Si (100) template for MOCVD applications,Opt. Express., 21 (2013) 26468-26474. https://doi.org/10.1364/OE.21.026468

[18] P.A. Gabrys, S.E. Seo, M.X. Wang, E. Oh, R.J. Macfarlane, C.A Mirkin, Lattice mismatch in crystalline nanoparticle thin films, In Spherical Nucleic Acids , Jenny Stanford Publishing, (2020) 1177-1193.

[19] Canham, L. Handbook of porous silicon , Springer, 2014.https://doi.org/10.1007/978-3-319-71381-6

[20] S.A.M. Salih, Porous Silicon Refractive Index Measurements with the Assistance of Two types of Lasers, Al-Nahrain J.Eng.Sci., 20 (2017) 1034-1039. https://doi.org/10.1002/1521-396X

[21] X. Kang, L. Wu, J. Xu, D. Liu, Q. Song, et.al. Preparation and photo-electrochemical properties of porous silicon/carbon dots composites, IOP Conf. Ser. Mater. Sci. Eng., 892 (2020) 012025. https://doi.org/10.1088/1757-899X/892/1/012025

[22] H.D. Jabbar, M.A. Fakhri, M.J. AbdulRazzaq, Synthesis Gallium Nitride on Porous Silicon Nano-Structure for Optoelectronics Devices, Silicon, 1-17,2022. https://doi.org/10.1007/s12633-022-01999-8

[23] F.T.L Muniz, M.R. Miranda, C. Morilla dos Santos, J.M. Sasaki, The Scherrer equation and the dynamical theory of X-ray diffraction, Acta Crystallogr. Sect. A: Found. Adv., 72 (2016) 385-390. https://doi.org/10.1107/S205327331600365X

[24] V.R. Kocharyan, A.S. Gogolev, A.E. Movsisyan, A.H Beybutyan, S.G. Khlopuzyan, L.R Aloyan, X-ray diffraction method for determination of interplanar spacing and temperature distribution in crystals under an external temperature gradient, J. Appl. Crystallogr., 48 (2015) 853-856. https://doi.org/10.1107/S1600576715006913

[25] T. Wang, X. LIa, W. Feng, W. LId, C. TAOd, J. WENa, Structure and photoluminescence properties of the quasi-regular arrangements of porous silicon, Optoelectron. Adv. Mater. Rapid Commun., 5 (2011) 495-498

[26] T. Tieu, M. Alba, R. Elnathan, A. Rius, N. Voelcker, Advances in porous silicon–based nanomaterials for diagnostic and therapeutic applications, Adv Ther., 2 (2019) 1800095. https://doi.org/10.1002/adtp.201800095

[27] K.H Li, C. Tsai, J. Sarathy, J.C. Campbell, Chemically induced shifts in the photoluminescence spectra of porous silicon, Appl. Phys. Lett., 62 (1993) 3192-3194. https://doi.org/10.1063/1.109126

[28] A.S. Hassanien, A.A. Akl, Effect of Se addition on optical and electrical properties of chalcogenide CdSSe thin films, Superlattices. Microstruct., 89 (2016) 153-169. https://doi.org/10.1016/j.spmi.2015.10.044

[29] C. Malerba, F. Biccari, C.L.A. Ricardo, M. D'Incau, P. Scardi, et.al. Absorption coefficient of bulk and thin film Cu2O. Solar energy materials and solar cells., 95(2011) 2848-2854. https://doi.org/10.1016/j.solmat.2011.05.047

[30] M.A. Fakhri, E.T. Salim, A.W Abdulwahhab, U. Hashim, et.al. Optical properties of micro and nano LiNbO3 thin film prepared by spin coating. Optics & Laser Technology., 103 (2018) 226-232. https://doi.org/10.1016/j.optlastec.2018.01.040

[31] A.S. Hassanien, A.A Akl. Optical characteristics of iron oxide thin films prepared by spray pyrolysis technique at different substrate temperatures, Appl. Phys. A., 124 (2018) 1-16. https://doi.org/10.1007/s00339-018-2180-6

[32] N.F. Mott, E.A Davis. Electronic processes in non-crystalline materials. Oxford university press, 2012.

[33] V. Džimbeg-Malčić, Ž. Barbarić-Mikočević, K. Itrić. Kubelka-Munk theory in describing optical properties of paper (I). Tehnički vjesnik., 18 (2011) 117-124.